

Solvatochromism of a Zwitterionic Benzimidazole-Based Pyridinium Betaine Dye: UV–Vis Spectroscopic Measurements and Quantum-Chemical Calculations

Juliusz Sworakowski,^{*,†} Józef Lipiński,^{*,†} Łukasz Ziólek,^{‡,§} Krystyna Palewska,^{*,†} and Stanislav Nešpůrek[§]

Institute of Physical and Theoretical Chemistry, Technical University of Wrocław, 50-370 Wrocław, Poland, and Institute of Macromolecular Chemistry, Academy of Sciences of the Czech Republic, 162 06 Prague, Czech Republic

Received: January 22, 1996; In Final Form: April 16, 1996[®]

The ground- and excited-state dipole moments of a zwitterionic benzimidazole-based pyridinium betaine dye [2,4,6-triphenylpyridinium-1-(1*H*-benzimidazol-2-ide), hereafter referred to as IB1] were determined. The ground-state dipole moment, calculated from measurements of the static electric permittivity of IB1 in 1,4-dioxane, exceeds 13 D units. The charge distribution in the molecule changes significantly upon excitation: the excited-state dipole moment, calculated from the solvatochromic shift of the low-energy UV–vis absorption band, is equal to ca. 3 D. The experimental results are supported by quantum-chemical calculations, which indicate that both the molecular geometry and positions of the energy levels are crucially influenced by solute–solvent interactions. The vectorial part of the second-order hyperpolarizability of IB1 molecules was estimated from the experimental data employing the two-state model: its off-resonance value amounts to ca. $-15 \times 10^{-40} \text{ m}^4/\text{V}$ ($-3.6 \times 10^{-30} \text{ esu}$).

1. Introduction

Among the methods allowing one to obtain information on parameters characterizing electronic properties of excited states, the simplest is that making use of the solvatochromic effect (e.g., refs 1–3 and references therein). The solvatochromic effect manifests itself as a shift of the positions of low-energy bands in electronic absorption and/or emission spectra of dissolved solute molecules, resulting from interactions with solvents of various polarity. In the case of molecules with sufficiently large ground-state permanent dipole moments, the solvatochromic shift observed in their UV–vis absorption spectra is primarily related to changes of the dipole moments upon excitation.^{1–3} In principle, measurements of the solvatochromic effect allow the determination of both the ground- and excited-state dipole moments (μ_g and μ_e , respectively). In addition, making use of the results of such spectroscopic measurements, one can also estimate the second-order hyperpolarizability of the solvatochromic molecule. All these parameters have been of interest to researchers studying molecular systems exhibiting nonlinear optical properties (cf., e.g., refs 4 and 5 and references therein).

In this paper, we report on measurements of the solvatochromism of a benzimidazole-based pyridinium betaine dye [2,4,6-triphenylpyridinium-1-(1*H*-benzimidazol-2-ide), hereafter referred to as IB1; cf. Figure 1]—a zwitterionic molecule belonging to the family of compounds whose best known representative is the so-called Reichardt's betaine dye,⁶ often used to scale empirically the polarity of solvents.^{2,7} The benzimidazole-based pyridinium betaine dyes are characterized by large ground-state dipole moments, exceeding 10 D (ref 8). Moreover, IB1 was expected to behave similarly to Reichardt's betaine dye, in which a significant decrease of the dipole moment upon excitation was observed.²

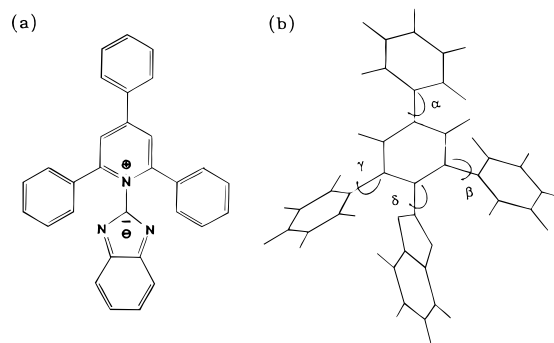


Figure 1. Molecular structure (a) and the conformation (b) of the IB1 molecule.

In our previous paper,⁹ we reported on the determination of the ground- and excited-state dipole moments, as well as the second-order hyperpolarizability of IB1. However, we observed a difference between the experimental results and quantum-chemical calculations performed for the free IB1 molecule, possibly resulting from solute–solvent interactions. In this paper, we put forward a more detailed analysis of the results, taking into account both the influence of the geometry of the solute molecule and the effect of the solvent on the electronic spectra of IB1.

2. Experimental Section

IB1 was synthesized at the Department of Organic Chemistry, Prague Institute of Chemical Technology, following the procedure described in detail elsewhere.¹⁰ The crude material was purified by multiple crystallization from chloroform and by chromatography on alumina, and its composition was checked by ¹H NMR and mass spectrometry. Purified IB1 was carefully dried immediately before the experiments. All solvents were of spectroscopic grade and were dried prior to use. The concentrations of solutions used in the experiments reported in this paper ranged between 10^{-5} and 10^{-4} mol/dm^3 . The results obtained with solvents which could possibly interact via specific

* To whom correspondence should be addressed.

† Technical University of Wrocław.

‡ Present address: Arthur Andersen Polska, 00-854 Warsaw, Poland.

§ Academy of Sciences of the Czech Republic.

® Abstract published in *Advance ACS Abstracts*, June 15, 1996.

interactions (e.g., alcohols) have not been included. Unfortunately, the number of solvents which could be used was additionally limited by insufficient solubility of IB1 in several nonpolar solvents (as well as in water). The absorption spectra were recorded using a UV-vis spectrophotometer Shimadzu 2101 PC; the relative electric permittivities of 1,4-dioxane solutions of IB1 were determined with a Tesla BM559 RLCG automatic bridge operating at 1 kHz. All measurements were carried out at room temperature.

3. Quantum-Chemical Calculations

The ground-state geometry of IB1 has been optimized using the AM1 method of Dewar et al.¹¹ Other parameters of IB1 (electronic transitions, polarization, dipole moments, etc.) have been evaluated using the GRINDOL method¹²—a modified version of an INDO-like approach including the configuration interaction (CI), with 500 singly excited configurations included in the procedure. The calculations were carried out for isolated IB1 molecules and for the molecules interacting with solvents.

Quantum chemical procedures which include a solvent effect have been well-known.^{13–16} Most of them introduce an energy operator of the solute molecule F in the form

$$F = F^0 + V \quad (1)$$

where F^0 stands for the energy operator of the free molecule and V is the energy of the electrostatic interactions between the solute and solvent molecules. Various methods have been employed, differing only in the choice of a detailed form of V . In the present work, the solvent effect was taken into account using a modified Langevin dipole (LD) model of Warshel and collaborators.^{16–19} Below, we shall give only a brief description of the modifications introduced in the original model; details of the method, as well as results of calculations of solvation energies, dissociation constants, solvatochromic shifts, and the effect of the solvent on nonlinear optical properties of molecules, will be given elsewhere.²⁰

Solvent molecules are represented in the LD model by a three-dimensional cubic grid of polarizable point dipoles constructed around the solute molecule as described in refs 16–19, each dipole (an i th molecule) being polarized by a local field resulting from a set of charges, dipoles, and quadrupoles located on atoms of the solute molecule,²¹ as well as from other solvent dipoles.

$$(E_i)^n = E_i^0 + (E_i^L)^n \quad (2)$$

In eq 2, E_i^0 is the field produced by the solute molecule (evaluated only once in a given series of calculations because the structure of the molecule has been fixed) and E_i^L is the field produced by other solvent molecules. The latter parameter is calculated self-consistently; $(E_i^L)^0 = 0$. In an n th iterative step, the polarization (expressed by the total dipole moment of an i th molecule) is approximated by the Langevin-type function given in eq 3

$$(\mu_i)^{n+1} = (\mathbf{e}_i)^n |\mu_s| [\coth z_i - z_i^{-1}]^n \quad (3)$$

where \mathbf{e}_i is the unit vector in the direction of \mathbf{E}_i , μ_s is the permanent dipole moment of the solvent molecules, and z is defined by eq 4

$$z_i = \frac{\mu_s \cdot \mathbf{E}_i}{kT} \quad (4)$$

In the modification of the method used in this paper, the electrostatic potential and electric field around the solute

molecule have been calculated using so-called cumulative atomic multipole moments (CAMP)²¹ obtained from the semiempirical wave functions of the GRINDOL method.¹² In this approach, each atom of the solute molecule is represented by a scalar net atomic charge, a vector of atomic dipole, and a tensor of atomic quadrupole.

In the LD model, the solvation free energy is dependent on the position and orientation of the solute molecule, placed in a cubic grid of polarizable solvent molecules. In the calculations reported in this paper, the optimum position and orientation of the solute molecule were determined using the Monte Carlo (MC) sampling method;²² hereafter, the modification of the model will be referred to as LD/MC technique. The maximum linear displacements (δr) and maximum rotation angle ($\delta \xi$) of the solute molecule (treated at this step as a rigid body) were chosen so as to bring the acceptance ratio near 0.5, in order to achieve a reasonable convergence. In most simulations, we used $\delta r = 0.005$ – 0.010 nm and $\delta \xi = 5$ – 10° . In each MC step, permanent and induced dipole moments of each solvent molecule, as well as the electric potential and electric field vector produced by all solvent molecules on each atom of the solute, were iteratively calculated using eqs 2–4. The average (in the meaning of the MC method) values of the electrostatic potential and electric field vector were incorporated into eq 1, and usual calculations with configuration interaction were carried out. The calculations were performed for IB1 interacting with either chloroform (a weakly polar solvent) or water (representing here a strongly polar solvent). In the latter case, the solvent was chosen for its simplicity: an almost total lack of solubility of IB1 in water makes it impossible to determine the spectra in this solvent. The number of solvent molecules taken into account in the calculations amounted to ca. 240 in case of chloroform and ca. 440 in case of water. Values of the input parameters of the LD/MC model are given in Table IS in the supporting information.

4. Results and Discussion

4.1. Ground-State Properties. *4.1.1. Dipole moment and dimerization of IB1.* The permanent ground-state dipole moment of IB1 was determined by measuring the relative electrical permittivity of dilute solutions of the solute in a nonpolar solvent (ϵ_{sol}) and calculating the concentration dependence of the molar polarizability of the solution²³ (Π_{sol}) according to eq 5

$$\Pi_{\text{sol}} = \frac{\epsilon_{\text{sol}} - 1}{\epsilon_{\text{sol}} + 2} \frac{M_{\text{sol}}}{\rho_{\text{sol}}} \quad (5)$$

where M_{sol} and ρ_{sol} are the molar mass and density of the solution, respectively. Assuming the molar mass and molar polarizability of the solutions to be additive functions of appropriate properties of the solute and solvent according to eqs 6a and 6b, one can determine the molar polarizability of

$$M_{\text{sol}} = x_s M_s + x_u M_u \quad (6a)$$

$$\Pi_{\text{sol}} = x_s \Pi_s + x_u \Pi_u \quad (6b)$$

the solute at infinite dilution: $\Pi_{u,0} = \lim_{x_u \rightarrow 0} \Pi_u$. In eqs 6a and 6b, x stands for the mole fraction of a component, the subscripts u and s referring to the solute and solvent, respectively. According to eq 7, the parameter $\Pi_{u,0}$ is believed to depend only on properties of solute molecules

$$\Pi_{u,0} = \Pi_{\text{dis}} + \frac{N_A \mu_g^2}{3\epsilon_0 kT} \quad (7)$$

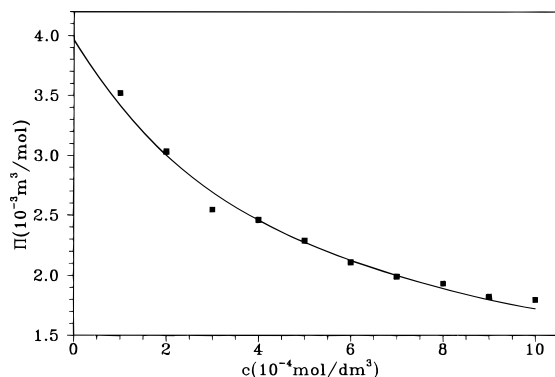
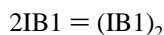


Figure 2. Concentration dependence of the molar polarizability of IB1 in 1,4-dioxane. The line represents a fit to the experimental results with the association constant amounting to 550.

where N_A is Avogadro's number, ϵ_0 is the permittivity of the free space, k is the Boltzmann constant, and Π_{dis} is the molar distortion polarizability of the solute molecule. The latter parameter is not too different from the molar refraction (R) and in most calculations is assumed equal to $(1-1.15)R$.

The molar polarizability of IB1 ($\Pi_{\text{u},0}$) was determined from the measurements of the static electric permittivities of solutions of IB1 in 1,4-dioxane; its average value was found to amount to $3.9 \times 10^{-3} \text{ m}^3/\text{mol}$ (cf. Figure 2). The molar refraction, estimated as a sum of structural increments,²⁴ is equal to $1.34 \times 10^{-4} \text{ m}^3/\text{mol}$. Thus, the ground-state dipole moment of IB1, calculated from these measurements, amounts to $(13.4 \pm 0.5) \text{ D}$, which is in reasonable agreement with both values given in the literature⁸ and the results of the quantum-chemical calculations given in the next section of this paper.

The molar polarizability of IB1 in its 1,4-dioxane solutions, shown in Figure 2, is clearly concentration-dependent. A phenomenon which may account for such an effect is the association of IB1, since strongly polar IB1 molecules are likely to form head-to-tail (and hence nonpolar) dimers, in equilibrium with monomers:



The apparent dipole moment (μ_t) is thus concentration-dependent and amounts to $\mu_g(1-y)$, y standing for the fraction of dimerized IB1 molecules. We attempted to estimate the dimerization constant of IB1 in 1,4-dioxane, at ambient temperature, assuming that the concentration dependence is solely due to the discussed effect. The association constant can be written as

$$K_d = \frac{c_D c^\square}{(c_M)^2} \quad (8)$$

where c_D and c_M are the molar concentrations of the dimer and monomer, respectively, and $c^\square = 1 \text{ mol/dm}^3$. After simple calculations, one arrives at eq 9

$$\mu_t = \frac{\mu_g c^\square}{4K_d c} \left[\left(1 + \frac{8cK_d}{c^\square} \right)^{1/2} - 1 \right] \quad (9)$$

with c being the nominal concentration of the solute. The obtained dependence, combined with eqs 7 and 8, allows one to fit the experimental results, with the dimerization constant as a parameter. The best fit was achieved for $K_d = 550 \pm 50$ (cf. Figure 2). Although K_d appears quite large, one should nevertheless realize that at concentrations used in our experiments (10^{-5} – 10^{-4} mol/dm^3), the fraction of dimerized molecules would be insignificant (of the order of a single percent at most); thus, possible UV-vis spectroscopic evidence for the existence of the dimers may be unavailable.

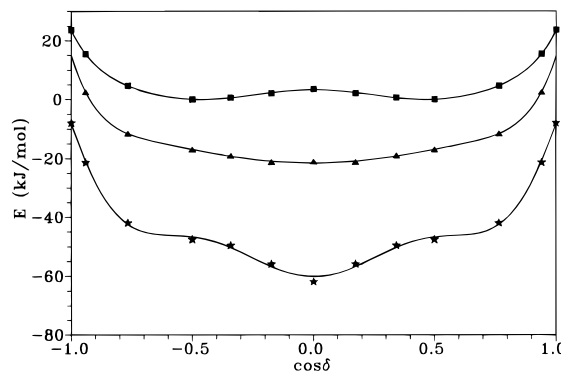


Figure 3. Dependence of the potential energy of the IB1 molecule on the dihedral angle δ : squares, isolated IB1 molecule; triangles, IB1 in chloroform; asterisks, IB1 in water. The zero of the energy scale has been set at the energy minima of an isolated molecule; the other curves have been displaced by the values of their solvation energies.

4.1.2. Molecular Geometry and Ground-State Dipole Moment Obtained from Quantum-Chemical Calculations. The IB1 molecule can be represented to a good approximation by a set of five rigid planar fragments (cf. Figure 1): the central pyridinium (Py) moiety, to which a benzimidazolyl (BI) and three phenyl rings (Ph1–Ph3) are attached. Thus, the conformation of IB1 is characterized by four dihedral angles (cf. Figure 1b): $\alpha(\text{Py-Ph1})$, $\beta(\text{Py-Ph2})$, $\gamma(\text{Py-Ph3})$, and $\delta(\text{Py-BI})$. Since the light-induced charge transfer occurs between the Py and BI moieties, the most important parameter is the dihedral angle δ ; as will be shown below, this parameter influences the energy and intensity of the transitions between the ground and low-lying excited states.

The influence of the geometry of the IB1 molecule was studied in the following cycle of calculations: having fixed a value of δ , we optimized the values of the remaining three angles and then computed the relevant parameters (the potential energy of the molecule, energies of the low-lying electronic states, transition strengths, dipole moments, etc.). The calculations were performed for an isolated IB1 molecule, as well as for the molecule interacting with a solvent (chloroform or water), using the procedure described in section 3 of this paper. In the case of an isolated molecule, the minimum of the potential energy is reached for $\delta \approx 60^\circ$, but the results shown in Figure 3 indicate that the potential energy curve is quite flat around the minima; i.e., the molecule enjoys a certain freedom of rotation around the Py–BI bond. The contribution of the solvation energy results in an important modification of the geometry of the molecule: the results of our calculations demonstrate that in both solvents the minimum of the potential energy is achieved at $\delta \approx 90^\circ$ (cf. Figure 3). It should also be noted that the shape of the potential energy curve depends on the solvent polarity: while in chloroform the curve is rather flat between ca. 40° and 140° , in water the minimum is much narrower and sharper. Consequently, one may deduce that the freedom of librations of the side groups of IB1 with respect to its central Py moiety should decrease with increasing solvent polarity. The optimized values of other angles calculated for the values of δ corresponding to minimum of the potential energy amount to $\alpha \approx -38^\circ$ (-37°), $\beta \approx 51^\circ$ (65°), $\gamma \approx -51^\circ$ (-65°); the values in parentheses were obtained for IB1 in solutions.

The ground-state dipole moment of IB1 is clearly environment- and conformation-dependent (cf. Figure 4); the values found for the optimized geometries of the molecule amount to 12.21, 14.24, and 15.86 D for an isolated molecule and for IB1 dissolved in chloroform and water, respectively. It should be noted that these values are in reasonable agreement with the

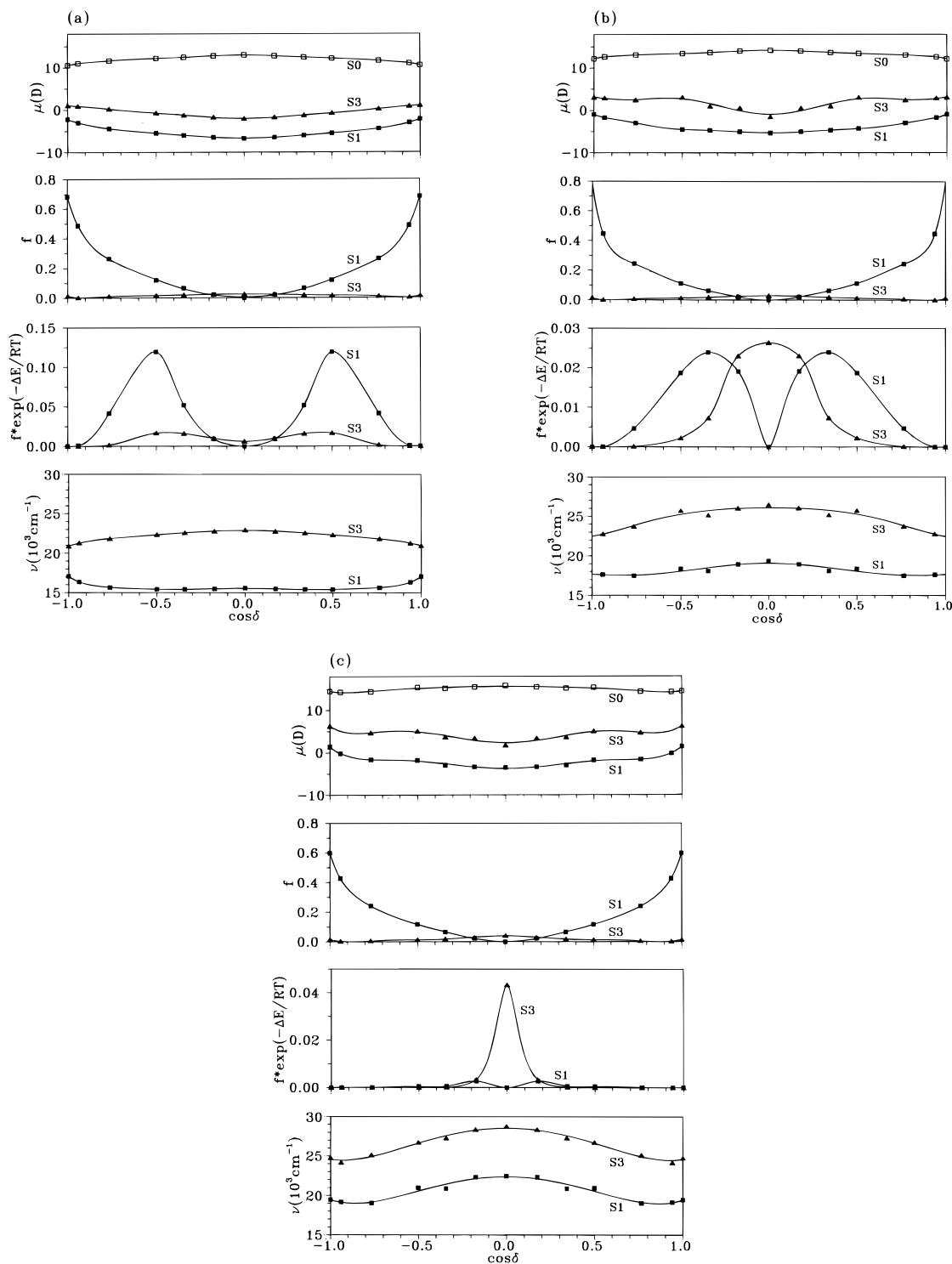


Figure 4. Dependence of the dipole moments of the IB molecule in the S_0 , S_1 , and S_3 states, and parameters of the $S_0 \rightarrow S_1$ and $S_0 \rightarrow S_3$ transitions, on the dihedral angle δ . (a) Isolated IB1 molecule; (b) IB1 in chloroform; (c) IB1 in water.

values given in the literature,⁸ as well as with the experimental result given in section 4.1.1.

4.2. Excited-State Properties. *4.2.1. Transition Energies and Oscillator Strengths.* As was already mentioned in our earlier paper,⁹ the UV-vis absorption spectrum of IB1 calculated for an isolated molecule contains medium- or low-intensity transitions below $22\,000\text{ cm}^{-1}$. The results of our calculations demonstrate that one can safely neglect the $S_0 \rightarrow S_2$ transition since its strength is insignificant irrespective of the molecular conformation (cf. Table IIS in the supporting information). Consequently, it is sufficient to take into account two lowest-lying ($S_0 \rightarrow S_1$ and $S_0 \rightarrow S_3$) transitions, which can be described

as intramolecular charge-transfer (CT) ones. The first strong absorption band appears at ca. $31\,000\text{--}32\,000\text{ cm}^{-1}$ and can be regarded as a superposition of a few close lying transitions, mostly confined to molecular moieties. While the position of the most intense transition appears in good agreement with the experiment (cf. Figure 6), our previous calculations⁹ resulted in underestimating the energy of the lowest-lying CT transition ($S_0 \rightarrow S_1$) and in overestimating its strength. We attribute this result to a strong dependence of the parameters of the CT bands on both the conformation and the environment of the absorbing molecule. It should be noted, however, that the results given in the preceding section indicate that the conformation of the

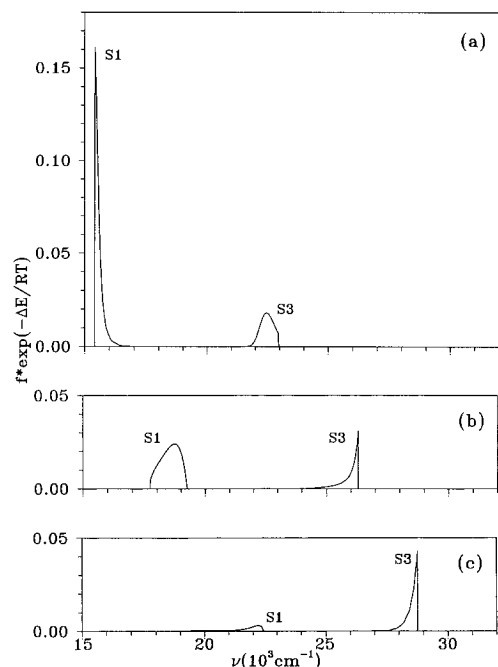


Figure 5. Energies and intensities of the low-energy transitions in IB1 calculated from the data of Figure 4. See text for further discussion.

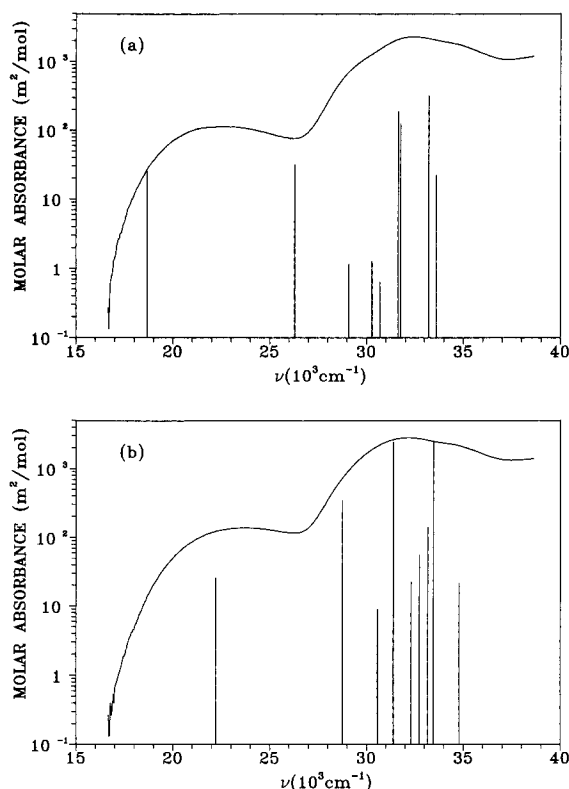


Figure 6. Absorption spectra of IB1 solutions in chloroform (a) and dimethyl sulfoxide (b). The vertical bars mark the energies of transition as obtained from the quantum-chemical calculations for IB1 dissolved in chloroform and water, their heights being proportional to the respective oscillator strengths. For the two lowest transitions, the heights of the bars are equal to the maximal values of the respective transitions shown in Figure 5.

molecule is strongly dependent on the presence of solvent. Thus one may expect changes in the calculated spectrum due to solute–solvent interactions.

It was shown in the preceding section that betaine molecules enjoy a certain freedom of rotation around the Py–BI axis. Since the energies and the oscillator strengths of the CT transitions

are conformation-dependent, one should expect a distribution of the latter parameters influencing the positions and bandwidths of the CT bands. Suitable calculations were carried out employing the GRINDOL method¹²: the energies ($\bar{\nu}$) of the S_1 and S_3 states, as well as the oscillator strengths (f) of the transitions to these states, were calculated in function of the dihedral angle δ (cf. Figure 4; see also the preceding section). These dependences can be combined into $[f(\delta) \exp(-\Delta E(\delta)/RT)]$ vs $\bar{\nu}(\delta)$ dependences, mimicking the effect of broadening of the absorption spectra by intramolecular librations around the Py–BI bond ($\Delta E(\delta) = E(\delta) - E_{\min}$, E_{\min} standing for the potential energy of the molecule in its equilibrium conformation). The results, shown in Figure 5, reveal that the interactions with the solvents are the primary cause of the shift of the low-lying absorption bands, the conformational changes of the solute molecules contributing to a lesser degree. On the other hand, the latter effect critically influences the intensities of the absorption bands and also contributes to their broadening. It should be noted that the minima of the potential energy of IB1 molecules in solvents are attained for $\delta \approx 90^\circ$, for which the oscillator strength of the $S_0 \rightarrow S_1$ transition is negligibly small (cf. also Table IIS). Thus it is the libration around the Py–BI bond which enables the observation of the latter transition: geometries with $\delta \neq 90^\circ$, although energetically less feasible, significantly contribute to the peak intensity.

4.2.2. Absorption Spectra. The UV–vis absorption spectra of IB1 in chloroform and dimethyl sulfoxide (representing weakly polar and strongly polar solvents, respectively) are shown in Figure 6. The main feature appearing in the spectral region covered by the experiments reported here (below 40 000 cm^{-1} , i.e., beyond the absorption region of the solvents used) is an intense band peaking at ca. 31 000 cm^{-1} , accompanied by a much weaker one at longer wavelengths. A comparison of the experimental results with those obtained from the quantum-chemical calculations (Figures 5 and 6; see also Table IIS) indicates that the long-wavelength absorption is due to the $S_0 \rightarrow S_1$ intramolecular CT transition, its transition moment directed along the long axis of the IB1 molecule (x axis). As indicated earlier, the strongest peak can be attributed to a superposition of transitions, mostly local in their character, possibly with some contribution from the $S_0 \rightarrow S_3$ and higher CT transitions hidden under the main peak. While the position of the main peak is influenced to a lesser degree by the nature of the solvent, the intensity and position of the weak CT band are strongly solvent-dependent: we observed a hypsochromic shift of the latter band on increasing the solvent polarity.

Due to a partial overlap of the bands, the position of the maximum of the CT absorption band was determined after fitting it with a Gaussian function, and its integral absorbance was then evaluated as twice the integral of the low-energy half of the experimental absorbance. The positions of maxima thus obtained, as well as the transition moments calculated from the integral absorbances, are listed in Table IIIS in the supporting information.

Theories describing the solvatochromic effect relate the band shift to weak interactions between a solute molecule and a solvent, usually treated as an isotropic dielectric medium characterized by its static relative electric permittivity (ϵ) and refractive index (n) (cf., e.g., refs 1–3 and 25 and references therein). The parameter taken as a measure of the shift is either the difference between the position of the lowest-energy absorption bands of an isolated molecule and that of the molecule dissolved in a given solvent (e.g. ref 26), or the difference between the positions of the lowest-energy absorption and fluorescence bands (e.g. ref 27). In this paper, we shall

employ eq 10 derived in ref 1, resulting from the model put forward by Abe²⁶

$$hc(\tilde{\nu}_A^s - \tilde{\nu}_A^0) = \frac{1}{4\pi\epsilon_0 a^3} [2\mu_g(\mu_g - \mu_e)(\varphi(\epsilon) - \varphi(n)) + (\mu_g^2 - \mu_e^2)\varphi(n)] \quad (10)$$

where $\varphi(\epsilon) = (\epsilon - 1)/(\epsilon + 2)$, $\varphi(n) = (n^2 - 1)/(n^2 + 2)$ and $\tilde{\nu}_A^s$ and $\tilde{\nu}_A^0$ are the wavenumbers corresponding to the CT absorption of an isolated solute molecule and the solute molecule in a solvent, respectively. The parameter a stands for the radius of a cavity (assumed spherical) occupied by the solute molecule. A plausible approximation for a , valid for $0.5r_u < r_s < r_u$, is¹

$$a = r_u + 0.5r_s \quad (11)$$

where r_u and r_s are the radii of the solute and solvent molecules, respectively, estimated from appropriate densities (ρ) and molar masses (M) according to eq 12

$$r_i = \left[\frac{3M_i}{4\pi\rho_i N_A} \right] \quad (i = u, s) \quad (12)$$

The values of a , calculated from eqs 11 and 12, vary between 0.666 and 0.697 nm (cf. Table IIIS). It should be noted that a confirmation of the choice of the latter parameter may be obtained from calculations of the solvent-accessible volume. Suitable calculations, carried out following the procedure described in ref 28, yield the value of 1.289 nm³; assuming the spherical shape of the molecule, the latter value is equivalent to $a = 0.675$ nm. Another assumption made on deriving eq 10 is the collinearity of μ_g and μ_e ; our calculations show that this condition is indeed fulfilled.

As comes from eq 10, the positions of the UV-vis band maxima should simultaneously be linear functions of $\varphi(n)$, and $[\varphi(\epsilon) - \varphi(n)]$, with the slopes being independent functions of μ_g and μ_e . Thus, in principle, the methods based on measurements of the solvatochromic shift allow for a simultaneous determination of μ_g and μ_e from the spectroscopic measurements only. However, the values obtained in this way are quite inaccurate. Therefore, we determined μ_g by measuring the static electric permittivity (cf. section 4.1.1.), using the spectroscopic results to determine only the excited-state moment. It is easy to demonstrate that the function $\varphi(n)$ varies very little between solvents (in the case of the solvents used in our experiments, $\varphi(n)$ ranges between 0.21 and 0.28); hence, eq 10 can be approximated by eq 10a. As appears from Figure 7, predictions

$$hc\tilde{\nu}_A^s = \frac{1}{4\pi\epsilon_0 a^3} [2\mu_g(\mu_g - \mu_e)(\varphi(\epsilon) - \varphi(n))] + \text{const} \quad (10a)$$

of the model are reasonably fulfilled. The excited-state dipole moment of IB1, calculated assuming $\mu_g = 13.4$ D (the value taken from the dielectric measurements), was estimated to amount to (3 ± 1) D.

On the basis of the results of the UV-vis spectroscopic measurements, one can also estimate the second-order hyperpolarizability of the molecule, employing the equations resulting from the sum-over-states quantum-mechanical model.^{29,30} Limiting oneself to the usual two-state model, one obtains eq 13 for the off-resonance value of the vectorial part of the hyperpolarizability tensor, directed along the direction of the charge transfer (the long axis of the molecule, in our case collinear with the directions of μ_g and μ_e)

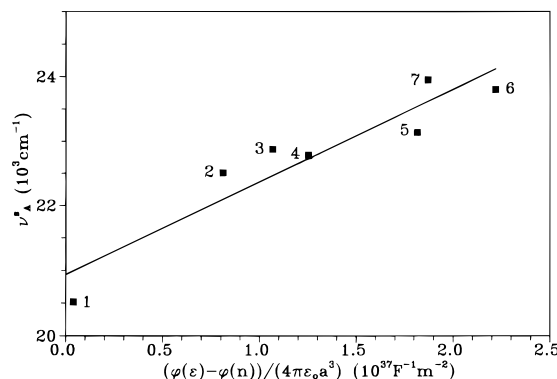


Figure 7. Dependence of the position of the low-energy UV-vis absorption band of IB1 on the solvent polarity. The numbering of the solvents: 1, tetrachloromethane; 2, chloroform; 3, ethyl acetate; 4, tetrahydrofuran; 5, acetone; 6, acetonitrile; 7, dimethyl sulfoxide.

$$\beta_{CT,0} = \frac{3\mu_{eg}^2(\mu_e - \mu_g)}{2\epsilon_0 h^2 c^2 (\tilde{\nu}_A^s)^2} \quad (13)$$

where μ_{eg} is the transition moment, related to the strength of the transition, which can be calculated from the integral absorbance given by eq 14^{30,31}

$$\int_{\text{band}} \epsilon(\tilde{\nu}) d\tilde{\nu} = \frac{2\pi^2 (\tilde{\nu}_A^s)^2 N_A \phi^2}{3 \ln 10 \epsilon_0 c h n} \mu_{eg}^2 \quad (14)$$

with $\epsilon(\tilde{\nu})$ being the molar absorbance appearing in the Lambert-Beer equation and ϕ —the local field factor—taken here in the Lorentz approximation as given by eq 15

$$\phi = \frac{n^2 + 2}{3} \quad (15)$$

The transition moment calculated from the above equations was found equal to ca. 2 D, depending on the solvent used (cf. Table IIIS). The values of $\beta_{CT,0}$, calculated assuming the applicability of the two-state model, for IB1 dissolved in chloroform and dimethyl sulfoxide (representing a weakly and strongly polar solvent, respectively) amount to -15.8×10^{-40} and -15.4×10^{-40} m⁴/V, respectively.

5. Final Remarks

The results of the measurements described in this paper yield a consistent picture. In the ground state, IB1 molecules exhibit a large permanent dipole moment exceeding 13 D, the experimental value being in a very good agreement with the results of the quantum-chemical calculations. There is a dramatic change in the dipolarity of the molecule upon excitation: the experimentally determined dipole moment of the molecule in its lowest-lying excited state is as low as ca. 3 D. This change is reflected in a considerable hypsochromic solvatochromic shift of the position of the intramolecular CT band of the IB1 dye with increasing solvent polarity (negative solvatochromism).

The experimental UV-vis absorption spectra of IB1 are in very good agreement with the calculated energies of the excited states in the region of the most intense band, i.e. around 31 000 cm⁻¹, where the dominant electronic transition is the local one. In the low-energy region, where a weak CT absorption band is observed, the calculations performed for an isolated molecule, reported in our previous paper,⁹ underestimated the energy of the excited states and overestimated the intensity of the $S_0 \rightarrow S_1$ transition. The results given in this paper clearly demonstrate

that a reasonable agreement can be achieved only after taking into account the solute–solvent interactions and the effect of the conformational changes.

It should not be left unmentioned that the calculated difference between the dipole moments in the S_0 and S_1 states significantly exceeds the experimental value of $\mu_g - \mu_e$. Apart from an inherently low accuracy of the solvatochromic method, the reason for this discrepancy should also be sought in the fact that the dipole moments of IB1 are influenced by the polarity of the solvent; thus, in reality they are not constant parameters as is assumed in the model used.

The hyperpolarizability of IB1, estimated from the two-state model, is about an order of magnitude lower than the values determined for typical molecular compounds exhibiting efficient second-order nonlinearity.³⁰ As can be inferred from eq 13, high hyperpolarizabilities can be found in materials in which a large transition moment is accompanied by an important change of the dipole moment upon transition. This is not the case with IB1: while the latter condition is indeed fulfilled, the intensity of the CT band (and hence the value of the transition moment) is far too low. We nevertheless believe that the structural flexibility of the betaine dye family opens ways to some molecular tailoring. Thus, design of a betaine molecule exhibiting a more intense CT transition (and hence an enhanced hyperpolarizability) is conceivable.

Acknowledgment. The authors are indebted to Professor J. Kuthan and Dr. S. Böhm (Prague Institute of Chemical Technology, Prague, Czech Republic) for the gift of betaine used in this work and stimulating discussions. One of the authors (J.L.) thanks Dr. A. Coser Gaudio (Universidade Estadual de Campinas, Brazil) for the computer program SURF. This work was supported by the Polish State Committee for Scientific Research (KBN Grant No. 2 P303 084 07).

Supporting Information Available: Tables containing parameters used in the LD/MC calculations; energies of excited states, oscillator strengths and transition moments of IB1; positions of the maximum of the absorption band of IB1 in various solvents (3 pages). Ordering information is available on any current masthead page.

References and Notes

- (1) Amos, A. T.; Burrows, B. L. In *Advances in Quantum Chemistry*; Academic Press: New York, 1973; pp 289–313.
- (2) Reichardt, Ch. *Solvents and Solvent Effects in Organic Chemistry*; VCH: Weinheim, 1988.
- (3) Liptay, W. In *Excited States*; Lim, E. C., Ed.; Academic Press: New York, 1974; pp 129–229.
- (4) Zyss, J.; Chemla, D. S., Eds. *Nonlinear Optical Properties of Organic Molecules and Crystals*; Academic Press: Orlando, FL, 1987.
- (5) Marder, S. R.; Sohn, J. E.; Stucky, W. D., Eds. *Materials for Nonlinear Optics, Chemical Perspectives*; American Chemical Society: Washington, DC, 1991.
- (6) Dimroth, K.; Reichardt, Ch.; Siepmann, T.; Bohlmann, F. *Justus Liebigs Ann. Chem.* **1963**, 661, 1.
- (7) Reichardt, Ch. *Chem. Rev.* **1994**, 94, 2319.
- (8) Alcalde, E.; Dinarés, I.; Elguero, J.; Fayet, J.-P.; Vertut, M.-C.; Miravittles, C.; Molins, E. *J. Org. Chem.* **1987**, 52, 5009.
- (9) Ziólek, L.; Palewska, K.; Lipiński, J.; Sworakowski, J.; Nešpůrek, S.; Böhm, S.; Meister, E. C. *Acta Phys. Pol. A* **1995**, 88, 283.
- (10) Böhm, S.; Kubík, R.; Němeček, J.; Kuthan, J. *Collect. Czech. Chem. Commun.* **1992**, 57, 1672.
- (11) Dewar, M. J. S.; Zebisch, E. G.; Healy, E. F.; Stewart, J. J. P. *J. Am. Chem. Soc.* **1985**, 107, 3902.
- (12) Lipiński, J. *Int. J. Quantum Chem.* **1988**, 34, 423.
- (13) Kollman, P. *Chem. Rev.* **1993**, 93, 2395.
- (14) Davis, M. E.; McCammon, J. A. *Chem. Rev.* **1990**, 90, 509.
- (15) Tomasi, J.; Persico, M. *Chem. Rev.* **1994**, 94, 2027.
- (16) Warshel, A. *Computer Modeling of Chemical Reactions in Enzymes and Solutions*; John Wiley: New York, 1991.
- (17) Lee, F. S.; Chu, Z. T.; Warshel, A. *J. Comput. Chem.* **1993**, 14, 161.
- (18) Luzhkov, V.; Warshel, A. *J. Am. Chem. Soc.* **1991**, 113, 4491.
- (19) Luzhkov, V.; Warshel, A. *J. Comput. Chem.* **1992**, 13, 199.
- (20) Lipiński, J.; Bartkowiak, W., in preparation.
- (21) Sokalski, W. A.; Poirier, R. A. *Chem. Phys. Lett.* **1983**, 98, 86.
- (22) Metropolis, N.; Rosenbluth, A. W.; Rosenbluth, M. N.; Teller, A. H.; Teller, E. *J. Chem. Phys.* **1953**, 21, 1087.
- (23) Minkin, V. I.; Osipov, O. A.; Zhdanov, J. A. *Dipole Moments in Organic Chemistry*; Plenum Press: New York, 1970.
- (24) Vogel, A. I.; Cresswell, W. T.; Jeffrey, G. H.; Leicester, J. J. *Chem. Soc.* **1952**, 514.
- (25) Koutek, B. *Collect. Czech. Chem. Commun.* **1978**, 43, 2368.
- (26) Abe, T. *Bull. Chem. Soc. Jpn.* **1965**, 38, 1314.
- (27) Bilot, L.; Kowski, A. *Z. Naturforsch.* **1962**, 17, 621.
- (28) Coser Gaudio, A.; Takahata, Y. *Comput. Chem.* **1992**, 16, 277.
- (29) Pugh, D.; Morley, J. O. Reference 3, Vol. 1, p 193.
- (30) Bosshard, Ch.; Sutter, K.; Prêtre, Ph.; Hulliger, J.; Flörsheimer, M.; Kaatz, P.; Günter, P. *Organic Nonlinear Optical Materials*; Gordon & Breach: Basel, 1995.
- (31) Barrow, G. M. *Introduction to Molecular Spectroscopy*; McGraw-Hill: New York, 1962.
- (32) Böttcher, C. J. F. *Theory of Electric Polarization*; Elsevier: Amsterdam, 1973; Vol. 1.

JP960184X